European Journal of Engineering and Applied Sciences

ISSN: 2651-3412 (Print) & 2667-8454 (Online)
Journal homepage: http://dergipark.gov.tr/EJEAS
Published by Çorlu Faculty of Engineering, Tekirdağ Namık Kemal University

European J. Eng. App. Sci. 8(1), 1-6, 2025

Araştırma Makalesi

The Effect Of Vacuum Heat Treatment On Microstructural And Corrosion Properties Of CuAl10Ni5Fe3Mn Alloy

Volkan Karakurt[1,a,*], Talip Çıtrak[1,b], Feyzanur Öztürk[1,c], Orçun Zığındere[1,d], Feriha Birol[1,e]

[1] Sağlam Metal San.ve Tic. A.Ş., R&D Department, Çayırova, Kocaeli, Türkiye, 41420
[a]volkan.karakurt@saglammetal.com, [b]talip.citrak@saglammetal.com, [c]feyzanur.ozturk@saglammetal.com,
[d]orcun.zigindere@saglammetal.com, [e]feriha.birol@saglammetal.com

Geliş: 13.06.2024 *Kabul: 03.02.2025* *DOI: 10.55581/ejeas.1500805*

Abstract: Nickel aluminum bronzes (NAB) are copper alloys widely used in critical applications in the defense, aerospace and marine industries. These alloys exhibit excellent properties such as wear resistance, corrosion resistance, impact strength, hardness and ductility, which are highly dependent on their composition and production conditions. Despite the relatively low formation of oxide layers on the surface of nickel aluminum bronze components under heat treatment conditions due to the high nickel content, there are special applications where the formation of oxide layers on the surface is undesirable. For this reason, the heat treatment of CuAl10Ni5Fe3Mn alloy was carried out in a vacuum furnace and the heat treatment process conditions in a non-vacuum muffle furnace were compared. For comparison purposes, the microstructure of the materials was examined and hardness and tensile tests and potentiodynamic corrosion tests were performed. It was determined that heat treatment in the muffle furnace led to a decrease in the proportion of the α phase and a higher formation of the β and κ phases compared to the heat treatment in a vacuum atmosphere. The material heat treated in the muffle furnace exhibited higher hardness and strength values as well as improved corrosion resistance compared to the material treated in the vacuum furnace.

Keywoards: *Nickel Aluminum Bronze, Vacuum Furnace, Muffle Furnace, Microstructure Characterization, Potentiodynamic Corrosion Behavior*

Vakum Isıl İşleminin CuAl10Ni5Fe3Mn Alaşımının Mikroyapısal ve Korozyon Özellikleri Üzerindeki Etkisi

Öz: Nikel alüminyum bronzları (NAB), savunma, havacılık ve denizcilik endüstrilerindeki kritik uygulamalarda yaygın olarak kullanılan bakır alaşımlarıdır. Bu alaşımlar, bileşimlerine ve üretim koşullarına büyük ölçüde bağlı olan aşınma direnci, korozyon direnci, darbe dayanımı, sertlik ve süneklik gibi mükemmel özellikler sergilerler. Yüksek nikel içeriği nedeniyle ısıl işlem koşullarında nikel alüminyum bronz bileşenlerin yüzeyinde nispeten düşük oksit katmanları oluşumuna rağmen, yüzeyde oksit katmanlarının oluşumunun istenmediği özel uygulamalar vardır. Bu nedenle CuAl10Ni5Fe3Mn alaşımının ısıl işlemi vakumlu fırında gerçekleştirilmiş ve vakumsuz kül fırınındaki ısıl işlem proses koşulları karşılaştırılmıştır. Karşılaştırma amacıyla malzemelerin mikro yapısı incelenerek sertlik ve çekme testleri ile potansiyodinamik korozyon testleri yapıldı. Kül fırınındaki ısıl işlemin, vakum atmosferindeki ısıl işleme kıyasla α fazının oranının azalmasına ve β ve κ fazlarının daha yüksek oluşumuna yol açtığı belirlendi. Kül fırınında ısıl işleme tabi tutulan malzeme, vakum fırınında işlem gören malzemeye göre daha yüksek sertlik ve mukavemet değerlerinin yanı sıra gelişmiş korozyon direnci sergilemiştir.

Anahtar kelimeler: *Nikel Alüminyum Bronzu, Vakum Fırını, Kül Fırını, Mikroyapı Karakterizasyonu, Potansiyodinamik Korozyon Davranışı*

* Corresponding author:
E-mail address: volkan.karakurt@saglammetal.com (V. Karakurt)

1. Introduction

Aluminum bronzes are widely used non-ferrous engineering materials. These materials contain 5-12% Al as the primary alloying element. Additions of iron, nickel and manganese make this alloy commercially available [1,2]. Nickel-containing aluminum bronze (NAB) casting alloys are increasingly used in areas where high strength, high impact properties and good corrosion resistance are required [2]. The addition of nickel increases the strength of the alloy without reducing its excellent ductility, toughness and corrosion resistance. The main areas of use of these alloys are valve seats, piston tips, marine engine shafts and aircraft components [1].

The mechanical, corrosion and abrasion properties of NAB alloys depend significantly on the types, sizes and amounts of phases present in their structure [3-7]. The composition of the alloy as well as the casting and heat treatment conditions determine the microstructure [7]. The typical casting microstructure of these alloys consists of a copper-rich α phase (matrix), a residual β phase (or β′ phase with a martensitic structure) depending on cooling conditions, intermetallic κ phases. Four different κ phases (κI, κII, κIII, κIV) with different compositions and morphologies have been determined in NAB alloys [8-9]. The κI phase is an iron-rich phase with a spherical or rosette morphology. The κII phase precipitates as dendritic rosettes, which are smaller than the κI phase, and is heterogeneously distributed at the α/β boundaries.

These two intermetallic phases are sensitive to the iron concentration in the alloy and the κII phase usually forms at lower iron concentrations, while the κI phase forms at higher iron concentrations (>5%). The κIII phase is formed at the α/β phase boundaries in a lamellar morphology, rich in nickel and aluminum. The κIV phase is an iron-rich intermetallic phase that precipitates in the matrix as fine precipitates [6-7].

The microstructure of NAB alloys is controlled by phase transformations that occur during heat treatment [6-7]. At temperatures above 1030 °C, NAB alloys have a β phase. As the temperature decreases, α phase starts to precipitate in the β phase. When the temperature drops to 930 °C, κII starts to precipitate from the β phase. At 860 °C, κIV precipitates from the α phase. When cooled below 800 °C, α+ κIII phase is formed from the residual β phase by eutectoid transformation. In addition to temperature, cooling rate also has an effect on microstructure. Under rapid cooling conditions, β′ phase transformation from β phase to occurs and this adversely affects the corrosion resistance of NAB alloy. For this reason, heat treatments applied to NAB alloys are usually performed at around 675 °C to remove the residual β phase [9].

Corrosion resistance in NAB alloys is provided by a protective oxide layer containing aluminum and copper oxide. This protective oxide layer consists of a copper oxide compound in the outer layer and an aluminum oxide compound in the inner layer. The κIII phase, rich in aluminum and nickel, contributes to corrosion resistance with the passive oxide layer it forms in the corrosive environment. While the α phase is a corrosion resistant phase in itself, it corrodes by forming a galvanic couple if it has an interface with κ phases with a more positive potential. The β′ phase is exhibits a sensitive characteristic to corrosion due to its stable martensitic structure and high chemical reactivity [9-15].

The main reasons for heat treatment of aluminum bronzes are to remove internal stresses, increase ductility, adjust tensile strength and hardness, improve corrosion resistance and wear resistance. Depending on the application, the alloy is subjected to various heat treatments such as stress relieving and solution annealing to achieve different levels of hardness and microstructure [5-9]. In the study by J.Böhm et al., the corrosion resistance of alloys cooled in different cooling media (Water and Air) and annealed at different annealing temperatures (700 °C and 500 °C) were comparatively investigated. As a result of the study, they stated that the β′ phase undergoes selective corrosion and that smaller and localized corrosion occurs with the separation of the β′ phase into α+ κ phases by annealing [16] . In another study, Z Qin et al. investigated the microstructure evolution and corrosion resistance of NAB alloy under different heat treatment conditions (annealing, normalizing, quenching and aging). As a result of the study, they found that selective corrosion occurs in the β′ phase in the complex microstructure containing α, κ and β′ phases in line with the literature. With the aging process at 450 °C, the microstructure was homogenized and corrosion was reduced by 50% [17].

Heat treatments are carried out in various environments and conditions, and in some cases where surface precision is required, they are also carried out in a vacuum environment. There are not many studies in the literature on the effect of heat treatment of aluminum bronzes in vacuum atmosphere on microstructure. In this study, the effects of heat treatment of a NAB alloy under vacuum and open atmosphere furnace conditions on the microstructure, hardness and corrosion properties of the material were investigated and compared.

2. Experimental

2.1. Materials

The CuAl10NiFe3Mn alloy used in the experimental studies was prepared in a 15 kg laboratory scale induction melting furnace at Sağlam Metal A.Ş. and then cast at 1100º C-1300º C range. The chemical analysis of the materials is given in Table 1. The castings were hot forged into bars using an open mold at 875°C.

Table 1. Chemical analysis of the sample

Chemical Composition (% Weight)				
Cu	Al	Ni	Fe	Mn
80.57	10.38	4.55	3.59	0.748

2.2. Heat Treatment Of The Materials

For comparison, the materials were heat treated in two different environments. The schematic graph of the heat treatment of the materials is given in Figure 1.

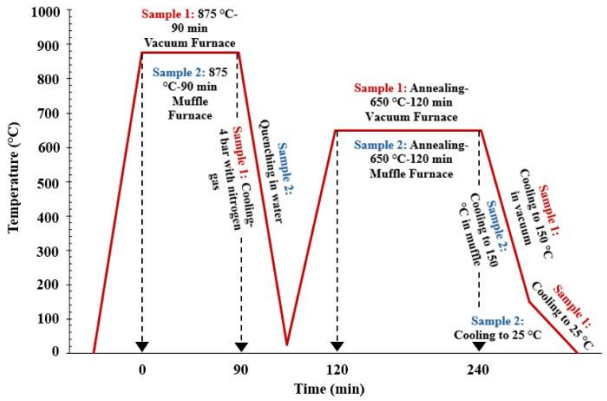

Figure 1. *Schematic heat treatment graph of the materials.*

Sample 1: After the samples were placed in the vacuum furnace at room temperature, the furnace temperature was raised to 875°C in 45 minutes, held at this temperature for 90 minutes, and then cooled to room temperature with 4 bar nitrogen gas under vacuum. Following this process, in the same environment, the vacuum furnace temperature was increased from room temperature to 650°C in 30 minutes, maintained at this temperature for 120 minutes, and then cooled to 150°C in the vacuum furnace. Finally, the samples were removed from the vacuum furnace and allowed to cool to room temperature. In this way, the quench and temper processes of the alloy were completed under vacuum. The vacuum furnace where the heat treatment was carried out is given in Figure 2.

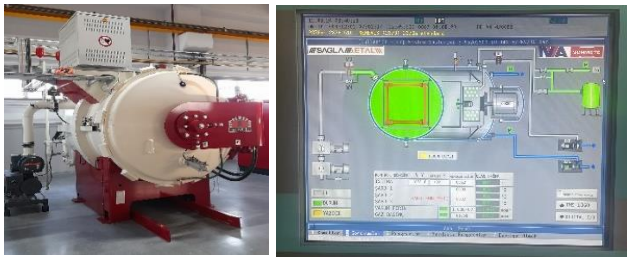

Figure 2. *Vacuum furnace where heat treatment of CuAl10Ni5Fe3Mn alloy takes place.*

Sample 2: In this condition, the thermal processes of the materials were carried out in an open atmosphere muffle furnace. After the samples were placed in the furnace, they were heated to 875°C in 45 minutes, held at this temperature for 90 minutes, and then rapidly quenched in water to cool to room temperature. Subsequently, they were heated from room temperature to 650°C in 30 minutes, held at this temperature for 120 minutes, and then allowed to cool in air after the temperature inside the furnace dropped to 150°C, completing the quenching and tempering processes. The muffle furnace where the heat treatment was carried out is given in Figure 3.

The microhardness values of all specimens were measured in vickers using Future-Tech FM800E microhardness tester under 1000 gf load applied for 10 seconds. Tensile tests of the materials were performed with INSTRON-3369 branded device. Samples for tensile tests were prepared according to ASTM E8/E8M-16a standard. Tensile tests were performed under a load of 50 kN and a speed of 50 MPa/s.

Figure 3. *Muffle furnace where heat treatments of CuAl10Ni5Fe3Mn alloy take place.*

In order to prepare the samples for metallographic examination, polishing was applied after sanding. The polished samples were immersed in a solution prepared with 50 ml HCl, 10 ml HNO_3, 10 g $FeCl_3$ and 100 ml distilled water, chemically etched and then prepared for microscopic examination. Microstructure examinations were carried out using a Nikon optical microscope and phase ratios were analyzed using Nikon Clemex Vision Lite software.

The corrosion rate of the samples was determined by electrochemical tafel extrapolation. Tafel curves were performed in 3.5% NaCl solution according to ASTM G59-97 standard using Gamry model PC4/300 mA potentiostat/galvanostat tester with DC105 software in accordance with ASTM G31-21 standard. A typical corrosion cell shown in Figure 3 was used for corrosion experiments. For the experiments, a copper wire connection was provided to the samples, molded with resin so that 10x10mm cross-sectional areas were exposed and connected to the opposite electrode in the cell to the atmosphere with a 150 mm long conductive copper cable (Figure 4).

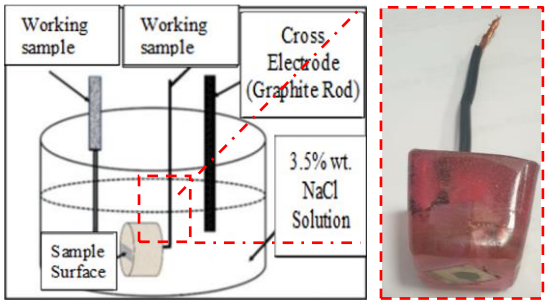

Figure 4. *Typical view of the cell and sample used in electrochemical corrosion experiments.*

A classical three-electrode cell was used with a graphite rod as the counter electrode, a saturated calomel electrode (SCE) as the reference electrode and the surface of the sample as the working electrode (Figure 3). Polarization curves were obtained by scanning in the range of -0.25 V and + 0.25 V with respect to the open circuit potential (Eoc) at a scan rate of 1 mVs^{-1}.

3. Results and Discussion

3.1. Microstructure Analysis

Optical microscope images and Clemex Vision Lite Image Analysis Software were used to characterize the phases formed

in CuAl10Ni5Fe3Mn alloy heat-treated under different conditions. The software identifies the phases of different structures in the microstructure in different colors according to the color tone difference. Accordingly, the software defined the stages in the structure in 3 different colors. Color image analysis of the samples subjected to heat treatment under vacuum and in an open-atmosphere muffle furnace with the help of an optical microscope and software is presented in Figure 4 (a-d). The microstructure and colored phase structure of the sample that was dissolved and annealed in a vacuum environment are presented in Figure 4 (a) and (b), and the images of the samples made in the muffle furnace are presented in Figure 4 (c) and (d). It is seen that the κ phases are more prominent in the heat treatments performed under vacuum (Figure 4 (a)), and the β phase is more dense in the sample heat treated in the atmospheric oven (Figure 4 (c)). As can be seen in Figure 4 (c), in addition to the β phase, a martensitic structure was formed in the sample heat treated in an open atmospheric furnace.

The results of the phase analysis ratios performed on the microstructure with the help of the Clemex program are given in Table 2. These analysis results enabled the differences and ratios between the microstructures to be quantified. According to this, the ratio of α, β and κ phases in the microstructure in vacuum environment is close to each other and 33.98% of this microstructure consists of α phase, 32.35% of β phase and 33.68% of κ phases. In the furnace open to atmosphere, these ratios changed and the ratio of α phase reached the lowest value (22.78%) and the ratio of κ phases reached the highest value (41.45%).

When the microstructures are compared, it is observed that heat treatment under vacuum leads to changes in the microstructure compared to heat treatment in an open atmosphere.

Table 2. Phase ratios results.

Phase Name	Vacuum Furnace % Phase analysis	Muffle Furnace % Phase analysis
Alfa (α)(green)	33.98	22.78
Beta (β) (blue)	32.35	35.77
Kappa Phases (κII, κIII, κIV) (red)	33.68	41.45

Microstructure images of the phase analysis are given in Figure 5. As a result of the phase analysis study, it was observed that the alpha phase was found at a higher ratio than the beta and kappa phases in the heat treatment performed in vacuum environment. It was understood that kappa and beta phases were found at a higher rate than alpha phase in the heat treatment performed in the muffle furnace and the values were compatible with the results in the literature [8]. It was observed that α-Cu matrix phase was present, κII phase was in spherical form, κIII phase was seen as a lamellar structure and finally κIV phase was seen as a point structure.

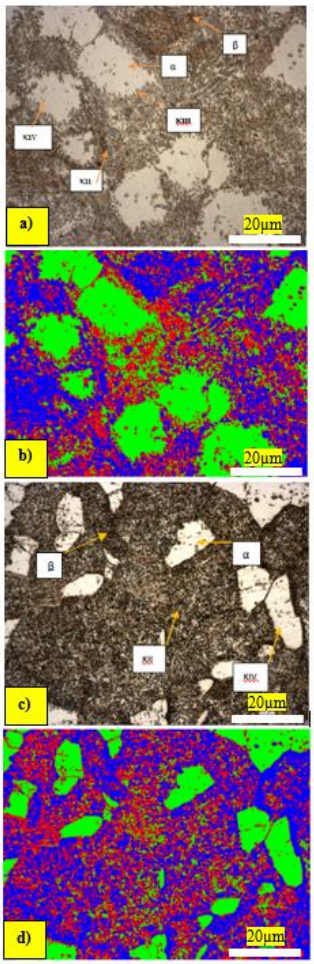

Figure 5. a) *Vacuum environments microstructure,* ***b)*** *Vacuum environments phase analysis, c) Muffle furnace microstructure,* ***d)*** *Muffle furnace phase analysis.*

3.2. Mechanical Test Results

The results of the hardness tests on materials subjected to heat treatment in both the vacuum furnace and the muffle furnace are presented in Figure 6, while the tensile test results are shown in Table 4. Examining Figure 6, it can be observed that the hardness of the CuAl10Ni5Fe3Mn alloy after heat treatment in the muffle furnace is 14 HV higher compared to the vacuum furnace heat treatment. Additionally, the tensile test results indicated that the CuAl10Ni5Fe3Mn alloy exhibited higher tensile and yield strengths under the muffle furnace heat treatment conditions compared to the vacuum furnace conditions. This is attributed to the faster cooling rate during the quenching process in the muffle furnace, whereas the cooling process was slower in the vacuum furnace. These different cooling regimes resulted in different phase formations, as shown in Table 2. In the muffle furnace heat treatment, the rapid quenching led to the formation of a darker β phase, resulting in a very hard and strong martensitic structure. The higher volume fraction of the β phase in the muffle furnace treatment, compared to the vacuum heat treatment, led to a greater increase in hardness and Strength [3].

Moreover, the dispersed kappa phase particles formed during the muffle furnace heat treatment impede dislocation

movement more effectively than in the vacuum heat treatment, making the material more resistant to deformation and thereby increasing its strength.

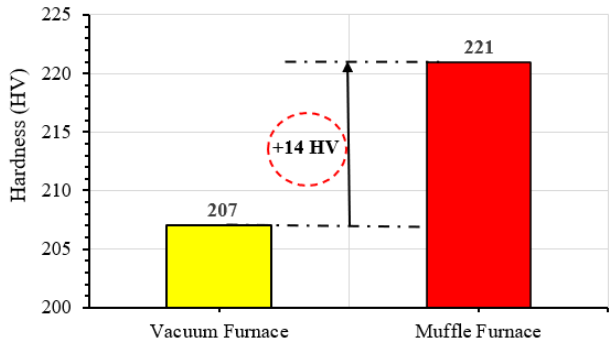

Figure 6. *Hardness values of materials.*

Table 4. Tensile test results.

Material Type	Yield Strength (MPa)	Tensile Strength (MPa)	Elongation %
Vacuum Furnace	359	741	29.4
Muffle Furnace	448	760	24.9

3.3. Corrosion Results

The Tafel curve obtained from the potentiodynamic corrosion results of samples heat-treated under different conditions in a 3.5% NaCl solution is shown in Figure 7. The corrosion potential, corrosion current density, and corrosion rate (mpy) are provided in Table 5.

According to the data, the corrosion properties of the CuAl10Ni5Fe3Mn alloy indicate that the heat treatment conducted in the muffle furnace provides superior corrosion resistance compared to the vacuum furnace. Specifically, the corrosion potential of the material treated in the muffle furnace is slightly more negative (-47.20 V compared to -45.40 V for the vacuum furnace), which typically indicates a higher tendency for initial corrosion. However, the significantly lower corrosion current density (13.20 x 10^{-6} A/cm² versus 17.60 x 10^{-6} A/cm²) and reduced corrosion rate (2.81 mpy versus 3.73 mpy) suggest that the alloy treated in the muffle furnace exhibits slower corrosion behavior. This enhanced performance can be attributed to the formation of a protective oxide layer on the surface during the muffle furnace heat treatment. In Figure 8, it is observed that the surface of the CuAl10Ni5Fe3Mn alloy treated in the muffle furnace appears darker, whereas no such darkening is observed on the material's surface after vacuum heat treatment. This darkening is presumed to be the oxide layer.

This oxide layer acts as a barrier, preventing further oxidation and thereby reducing the overall corrosion rate. Additionally, the rapid quenching process in the muffle furnace, compared to the slower cooling rate in the vacuum furnace, results in a higher density of kappa phase, which is considered to impact corrosion resistance. The higher amount of kappa phase, particularly rich in Ni_3Al, formed during the muffle furnace treatment enhances the alloy's resistance to corrosion [18-19]. Therefore, heat treatment in the muffle furnace provides superior corrosion due to the formation of the oxide layer and higher kappa phase content.

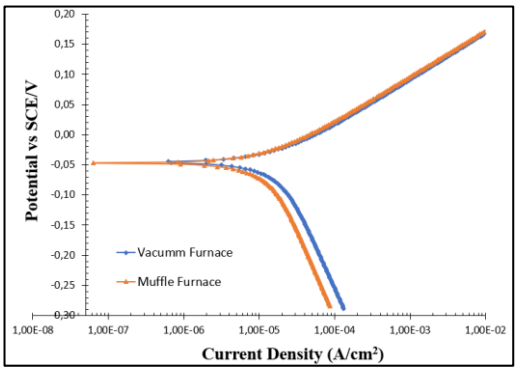

Figure 7. *Potentiodynamic Tafel curves of materials heat treated in vacuum and muffle furnace.*

Table 5. Potentiodynamics Corrosion test results.

Material Type	Corrosion Potential (V)	Corrosion Current Density (Icorr., A/cm²)x10^{-6}	Corrosion Rate (mpy, thickness reduction in miles per year)
Vacumm Furnace	-45.40	17.60	3.73
Muffle Furnace	-47.20	13.20	2.81

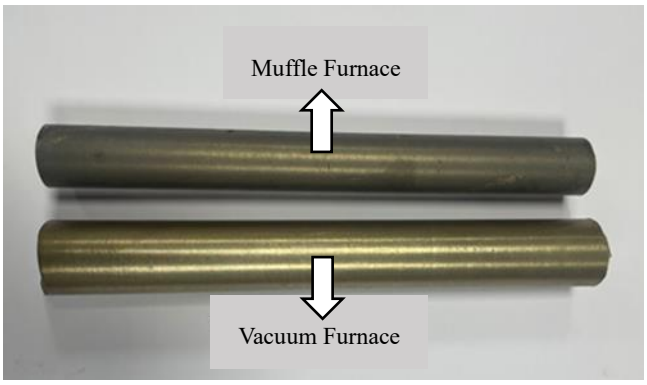

Figure 8. *Surfaces of materials*

4. Results

- Thermal treatments in both vacuum and muffle furnace environments changed the microstructure of the CuAl10Ni5Fe3Mn alloy. These changes were attributed to differences in cooling rates.
- The heat treatment in the muffle furnace resulted in a decrease in the α phase and an increase in the β and kappa (κ) phase compared to the vacuum atmosphere heat treatment.

- Increasing the β and κ phase ratios in the microstructure improved the mechanical properties of the alloy processed in the muffle furnace, resulting in higher hardness and strength values.
- Vickers hardness measurements showed that the material heat treated in the muffle furnace had a hardness of 14 HV higher than the material heat treated in vacuum.
- Potentiodynamic polarization test results showed that the material heat treated in the muffle furnace exhibited higher corrosion resistance compared to the material heat treated in vacuum. The superior corrosion resistance of the muffle furnace heat-treated material is attributed to the formation of the oxide layer and the presence of kappa phases rich in Ni_3Al.

Author Contribution

Investigation, writing, review, explanation of corrosion mechanisms-Volkan Karakurt; Writing-original draft, Methodology-Talip Çıtrak; Experimental Performance-Feyzanur Öztürk; Writing-review and editing-Orçun Zığındere; Review and Editing, Conceptualization-Feriha Birol

Declaration of Competing Interest

The authors declared no conflicts of interest with respect to the research, authorship, and/or publication of this article.

References

[1] Meigh, H. (2018). Cast and wrought aluminium bronzes: properties, processes and structure. CRC Press.

[2] Culpan, E. A., & Rose, G. (1978). Microstructural characterization of cast nickel aluminium bronze. Journal of materials science, 13, 1647-1657.

[3] Brona, M. L. A. (2014). Influence of heat treatment on the microstructure and mechanical properties of aluminium bronze. Mat. Technol, 48, 599-604.

[4] Jahanafrooz, A., Hasan, F., Lorimer, G. W., & Ridley, N. (1983). Microstructural development in complex nickel-aluminum bronzes. Metallurgical Transactions A, 14, 1951-1956.

[5] Meigh, H. (2018). Cast and wrought aluminium bronzes: properties, processes and structure. CRC Press.

[6] Hasan, F., Jahanafrooz, A., Lorimer, G. W., & Ridley, N. (1982). The morphology, crystallography, and chemistry of phases in as-cast nickel-aluminum bronze. Metallurgical Transactions A, 13, 1337-1345..

[7] Ünal, M. "Alüminyum bronzunda farklı katılaşma hızlarının mikroyapı ve mekanik özelliklerine etkisi, (1999), MsC, Gazi Üniversitesi Fen Bilimleri Enstitüsü, Ankara.

[8] Yaseen, M. K., Mansoor, M., Ansari, H. A., Hussain, S., & Khan, S. (2018). Effect of heat treatment on tribological characteristics of CuAl10Ni5Fe4 nickel aluminum bronze. Key Engineering Materials, 778, 61-67.

[9] Zhang, D., Ruiping, C. H. E. N., Zhang, W., Zongqiang, L. U. O., & Yuanyuan, L. I. (2010). Effect of microstructure on the mechanical and corrosion behaviors of a hot-extruded nickel aluminum bronze. Acta Metallurgica Sinica (English Letters), 23(2), 113.

[10] H. S. Campbell, "Aluminium Bronze Corrosion Resistance Guide," Publication 80, Copper Development Association, UK, July 1981, pp. 1-27.

[11] Anantapong, J., Uthaisangsuk, V., Suranuntchai, S., & Manonukul, A. (2014). Effect of hot working on microstructure evolution of as-cast Nickel Aluminum Bronze alloy. Materials & Design, 60, 233-243.

[12] Orzolek, S. M., Semple, J. K., & Fisher, C. R. (2022). Influence of processing on the microstructure of nickel aluminum bronze (NAB). Additive Manufacturing, 56, 102859.

[13] Wu, Z., Cheng, Y. F., Liu, L., Lv, W., & Hu, W. (2015). Effect of heat treatment on microstructure evolution and erosion–corrosion behavior of a nickel–aluminum bronze alloy in chloride solution. Corrosion Science, 98, 260-270.

[14] Ding, Y., Zhao, R., Qin, Z., Wu, Z., Wang, L., Liu, L., & Lu, W. (2019). Evolution of the corrosion product film on nickel-aluminum bronze and its corrosion behavior in 3.5 wt% NaCl solution. Materials, 12(2), 209.

[15] Wharton, J. A., Barik, R. C., Kear, G., Wood, R. J. K., Stokes, K. R., & Walsh, F. C. (2005). The corrosion of nickel–aluminium bronze in seawater. *Corrosion science*, *47*(12), 3336-3367.

[16] Böhm, J., Linhardt, P., Strobl, S., Haubner, R., & Biezma, M. V. (2016). Microstructure of a heat treated nickel-aluminum bronze and its corrosion behavior in simulated fresh and sea water. Materials Performance and Characterization, 5(5).

[17] Qin, Z., Zhang, Q., Luo, Q., Wu, Z., Shen, B., Liu, L., & Hu, W. (2018). Microstructure design to improve the corrosion and cavitation corrosion resistance of a nickel-aluminum bronze. Corrosion Science, 139, 255-266.

[18] Huttunen-Saarivirta, E., Isotahdon, E., Metsäjoki, J., Salminen, T., Carpén, L., & Ronkainen, H. (2018). Tribocorrosion behaviour of aluminium bronze in 3.5 wt.% NaCl solution. Corrosion Science, 144, 207-223.

[19] Powell, C., & Webster, P. (2019). Copper alloys. In Corrosion Performance of Metals for the Marine Environment EFC 63 (pp. 26-41). CRC Press.